Journal of Food Science and Technology (Iran)

Homepage: www.fsct.modares.ir

Scientific Research

# Experimental Study on Chicken meat Thawing Using Hybrid High-Voltage Electric Field and Infrared Technology: Investigating the Effects of Reflector Configuration and Infrared Source Distance

**Mohsen Dalvi-Isfahan[1*], Hamid Khafajeh[2*]**

1-Department of Food Science and Technology, Faculty of Agriculture, Jahrom University, Jahrom, Iran

2-Department of Mechanical Engineering of Biosystems, Jahrom University, Jahrom, Iran

**ARTICLE INFO**

**Article History:**

Received: 2026/02/25

Review: 2026/05/13

Accepted: 2026/05/20

**Keywords:**

Thawing,

Electric Field,

Infrared,

Chicken Meat,

Tissue Quality,

Specific Energy Consumption

DOI: **10.48311/fsct.2026.119582.83083**

*Corresponding Author E-

Dalvi@jahromu.ac.ir,
mohsen.Dalvi@gmail.com

khafajeh@jahromu.ac.ir

**ABSTRACT**

In this study, to overcome the limitations of conductive heat transfer, the performance of a hybrid system consisting of infrared radiation and an electric field with an intensity of 6/7 kV/cm was evaluated for thawing frozen chicken fillets. The studied variables included reflector type (matte, glossy, and mesh) and the radiation source distance at three levels. Their effects on thermal kinetics, specific energy consumption, weight loss, and color parameters were assessed. The results showed that the optical properties of the reflector play a significant role in the uniformity of heat flux. The matte reflector, by producing diffuse reflection, reduced the thawing time to approximately 12 minutes and decreased energy consumption to 13 kJ/g, while preventing hot spot formation and preserving surface lightness. In contrast, the mesh reflector increased the process time to about 22 minutes due to greater energy losses. Moreover, the higher intensity of radiative heat transfer in the matte reflector resulted in the greatest weight loss, whereas the mesh reflector, with milder heating, exhibited the lowest weight loss and better moisture retention. Evaluation of the radiation source distance also revealed a nonlinear behavior dependent on the view factor. A distance of 14 cm led to thermal saturation and deterioration of color quality, while a distance of 17 cm provided a balance between radiation intensity and heat penetration, preserving color and minimizing weight loss. Overall, the combination of a matte reflector and a 17 cm distance provided the most efficient ecothermodynamic conditions.

## 1-Introduction

Chicken meat, as one of the most strategic and widely consumed sources of protein in household diets worldwide, plays a vital role in ensuring food security. In our country as well, according to official statistics and an annual production exceeding 3 million tons of chicken meat, this product accounts for a major share of the protein products market [1]. Managing such a vast volume of production and its distribution across a wide geographical area requires an efficient chain of preservation processes, at the forefront of which is freezing. Freezing reduces the product temperature below the freezing point of water and converts free water into ice crystals, thereby lowering water activity and, by slowing biochemical reactions and inhibiting microbial growth, enabling long-term storage and stabilization of market fluctuations. However, the final quality of the product that reaches the consumer or enters the industrial processing cycle is not determined solely by the freezing process; rather, the thawing stage represents the primary bottleneck and the most critical point in the value chain of frozen meat [2].

During freezing, ice crystals are formed, and if conditions are not properly controlled, large and sharp crystals may develop. These large crystals rupture the walls of muscle cells and protein membranes, thereby disrupting the natural structure of the meat tissue. The direct consequence of this damage is the reduced capacity of the tissue to reabsorb intercellular water after ice melting, which manifests as the phenomenon known as drip loss. The release of drip loss not only results in product weight reduction and significant economic losses for producers, but also leads to the loss of a considerable portion of soluble proteins, vitamins, minerals, and flavor compounds, ultimately yielding a dry, tough product with diminished nutritional value [3].

At present, a substantial portion of the food industry—as well as household applications—continues to rely on traditional thawing methods, such as refrigeration, exposure to ambient air, or immersion in water. These approaches are primarily based on conductive heat transfer from the surface to the core of the product. Since the thermal conductivity of water, approximately 0.6 W/m·K, is nearly four times lower than that of ice, approximately 2.2 W/m·K, the melting of the outer layers of meat leads to the formation of an insulating layer of liquid water around the product. This layer inhibits the rapid transfer of heat to the still-frozen core. Such a physical phenomenon significantly prolongs the overall thawing process. Prolonged thawing time has two critical consequences: first, a substantial deterioration in texture quality due to lipid oxidation and protein denaturation; and second—and of greater sanitary importance—the extended exposure of the product surface to the temperature danger zone (5 to 60°C). This temperature range provides ideal conditions for the reactivation and exponential growth of pathogenic microorganisms such as *Salmonella*, *Campylobacter*, and *Escherichia coli*, which can endanger consumer health. Moreover, methods such as water immersion consume large volumes of water and generate contaminated wastewater, thereby creating serious environmental challenges [4].

In order to overcome the inherent limitations of conventional thawing methods, extensive research over recent decades has focused on the development of emerging technologies. The primary objectives of these technologies are to reduce processing time, achieve uniform heating, minimize drip loss, and ensure microbial safety. Among the broad spectrum of innovative approaches—including ultrasound, microwave, radio frequency, and high-pressure treatments—two technologies, namely high-voltage electric field and infrared radiation, have attracted particular attention due to their distinct physical mechanisms and significant industrial potential.

High-voltage electric field technology is a novel non-thermal method based on the application of a high voltage (typically in the kilovolt range) between a discharge electrode (needle or wire) and a grounded electrode. The mechanism underlying its effectiveness in thawing is complex and multifaceted, and can be categorized into two main groups: external dynamic effects and internal molecular effects. This method has been successfully applied by various researchers for thawing a range of products, including poultry, fish, and pork [5–7].

In addition to electric fields, infrared heating has been introduced as an efficient thermal method. Unlike convective methods, which require heating an intermediate medium such as air, infrared waves transfer energy directly to the surface of the product through radiation at the speed of light. Upon striking the surface of the meat, these waves are absorbed, causing molecular vibrations and subsequent heat generation. The main advantage of infrared heating lies in its very high heat transfer rate and the relative simplicity of its equipment. However, the major limitation of this method is its low penetration depth, meaning that the energy is primarily absorbed at the surface. This characteristic may lead to excessive surface heating (even localized cooking) while the core of the product remains frozen [8]. Davoodi et al. (2018) investigated the effect of a combined infrared–hot air method on the quality characteristics of ground chicken meat. The results indicated that increasing parameters such as radiation power, air temperature, and air circulation velocity significantly enhanced the thawing rate. Using response surface methodology, the optimal conditions were determined to be a radiation power of 247.73 W, an air temperature of 38.97 °C, and an air circulation velocity of 6.75 m/s [9].

In this study, the simultaneous effects of an electric field and infrared radiation on the thawing process are investigated. In this combined system, infrared radiation provides the thermal energy required for rapid ice melting, while the electric field plays a complementary role by enhancing heat transfer. The infrared method relies on radiative heat transfer, whereas the electric-field-based method primarily depends on convective heat transfer. In addition to the thermal effects generated by the ion wind phenomenon, non-thermal mechanisms also contribute to heat transfer in the electric field, thereby accelerating the thawing process. The application of an electric field disrupts the thermal boundary layer and enhances heat transfer, facilitating and accelerating the thawing process [10].

The non-thermal mechanisms of the electric field, including the direct action of the field on water molecules, induce changes in their orientation and weaken hydrogen bonds, which in turn reduces ice crystal size and accelerates their melting. Moreover, the generation of reactive oxygen and nitrogen species through this method can alter the structure of meat proteins, improving tissue quality and water-holding capacity [11].

Recent studies have also shown that the electrokinetic forces generated by the electric field in moist materials enhance fluid movement and convective mass transfer, contributing to temperature uniformity and further accelerating the thawing process. Consequently, it is expected that the combination of an electric field and infrared radiation can increase the thawing rate while reducing structural damage to the meat [12]. The overall outcome of this synergistic interaction is a process that not only achieves significantly higher speed, but also preserves the texture quality (water-holding capacity), sensory attributes (color and flavor), and microbial safety of chicken meat at an optimal level. This combined approach opens new horizons in the food processing industry and promises a transition from inefficient traditional methods toward intelligent, energy-efficient, and high-quality systems in the near future. In this study, by keeping the electric field conditions constant, we focus on examining the effects of the infrared-based method parameters.

## 2- Materials and Methods

### 2.1. Sample Preparation

Fresh skinless and boneless chicken breast fillets were procured daily. The chicken samples were cut into uniform cubes (2×2×2 cm) and rapidly frozen in a freezing tunnel at −30°C with an air velocity of 1 m/s1 for approximately 2 h, until the core temperature reached about −8°C. Immediately after freezing, the samples were vacuum-packaged in polyethylene bags and stored at −18°C for no longer than one week prior to the experiments, in order to minimize quality changes associated with prolonged storage [6].

### 2.2. Experimental Procedure

The experimental apparatus consisted of a high-voltage power supply connected to a voltage controller, capable of providing voltages up to 20 kV. The system employed a wire-to-plate electrode configuration positioned a treatment chamber. The grounded electrode consisted of a flat rectangular copper plate measuring 15×20 cm, while several parallel wire electrodes (connected to the positive terminal of the power supply) were suspended 3 cm above the plate, generating a non-uniform electric field with an average field strength of 6.7 kV/cm throughout the treatment zone. Chicken meat samples were placed directly on the grounded electrode inside the chamber.

An infrared lamp (model BR125, Philips, Eindhoven, the Netherlands) with a power rating of 250 W was installed above the electrode assembly to provide simultaneous thermal energy. In order to evaluate the effect of different radiation levels, three distances between the infrared source and the sample surface (14, 17, and 20 cm) were tested in this study. In addition, to enhance heat transfer and better simulate realistic thawing conditions, a convective airflow at 20°C with a velocity of 0.4 to 0.5 m/s was maintained inside the incubator. The air velocity inside the chamber was measured using a hot-wire anemometer (model Testo 405i, Testo, Germany). A schematic diagram of the system used in this study is presented in Figure 1.

To investigate the thermal kinetics of the thawing process, the temperature at the thermal center of the samples was continuously monitored. Temperature changes at the sample center were recorded using type K thermocouples connected to a data logger. These data were used to analyze the temperature profile, determine the heating rate, and examine kinetic differences arising from reflector type and radiation source distance. The thawing process was considered complete when the temperature at the coldest point of the sample (thermal center) reached a value slightly above the freezing point of the food product [6].

In this study, three different types of reflectors—matte, glossy, and mesh—were used. These reflectors served as the grounded electrode in the present system while also functioning as infrared reflectors, and they are shown in Figure 2. Based on the findings of Davoodi et al. (2018), who identified a power level of approximately 250 W as suitable for thawing chicken samples, this power was considered a constant parameter in the present study [9]. In contrast, the distance between the light source and the sample was selected as the variable under investigation. The importance of this variable lies in determining the optimum distance in terms of the view factor in radiative heat transfer, which can have a substantial influence on thawing efficiency. Since the view factor affects the amount of radiation transferred from the source to the sample surface, optimizing the radiation distance can significantly improve the overall process efficiency.

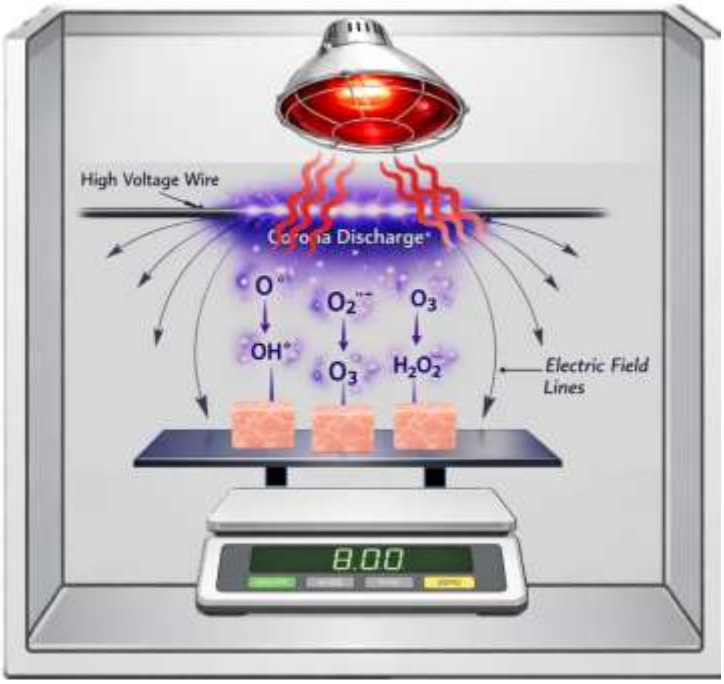


Figure 1. Schematic of the hybrid thawing device (combination of infrared and electric field).

a b c

Figure 2. Types of reflectors used in this study: (a) matte, (b) glossy, and (c) mesh.

**2.3. Weight Loss**

Weight loss was determined by measuring the difference in mass between the frozen sample and the same sample after thawing. The percentage of weight loss for each treatment was calculated based on the recorded initial and final weights of the samples.

**2.4. Color Measurement**

To evaluate the surface color of the meat, images were captured both before freezing and immediately after the completion of the freezing–thawing process. A digital camera (Canon PowerShot A540, Canon, Tokyo, Japan) with a resolution of 6 megapixels was used for image acquisition. The samples were placed inside a wooden box illuminated by two daylight-simulating lamps to ensure uniform lighting conditions and to minimize variations caused by ambient light. The obtained images were analyzed using ImageJ software to quantify the CIE color parameters L*, a*and b* [13].

**2.5. Measurement and Calculation of Specific Energy Consumption**

Energy consumption in this system was determined by calculating the total electrical power consumed by the heating and electrical components during the thawing process. The total energy consumption was considered as the sum of the energy used by the infrared lamp and the high-voltage power supply. The power consumption of the infrared lamp was assumed to be equal to its nominal power (250 W), while the power consumption of the high-voltage system was calculated as the product of the applied constant voltage (20 kV) and the electric current passing through the circuit, which was monitored by an ammeter integrated into the power supply.

By multiplying the total power consumption by the exact duration of the thawing process, the total energy consumption was obtained in joules or kilojoules. Finally, to standardize the results and eliminate the effect of slight variations in sample mass, the specific energy consumption index was calculated by dividing the total energy consumed by the initial mass of the frozen meat sample and expressed in units of kJ/g [14].

### 2.6. Statistical Analysis

The experiments were designed sequentially based on a one-factor-at-a-time (OFAT) approach, in which only one variable was changed at each stage while all other variables were kept constant in order to evaluate the independent effect of that factor. According to this design, in the first phase three types of reflectors were examined while keeping the distance constant. In the second phase, with a selected reflector type kept constant, the effect of the radiation source distance was investigated at three different levels.

Each experiment was performed in triplicate, and the results were reported as mean ± standard deviation in tables and figures. Statistical analyses were conducted using SPSS software (version 27). Data evaluation was performed using one-way analysis of variance (ANOVA), and differences between treatment means were determined using Duncan's multiple range test at a 95% confidence level ($P<0.05$).

## 3-Results and Discussion

### 3.1. Effect of Reflector Type on Thawing Time and Temperature Profile

Figure 3 illustrates the effect of the reflector type (which also served as the ground electrode in this system) on the thawing time of the samples. The results indicate that the optical properties and surface structure of the reflector significantly influenced the heat transfer rate and the reduction of thawing time. Reflector type A (matte surface) exhibited the highest efficiency, recording the shortest thawing time (approximately 12±3 min) ($P < 0.05$). This superior performance can be attributed to the higher emissivity and the diffuse reflection characteristics of matte surfaces, which allow the radiative energy to be redistributed more uniformly and effectively over the entire surface of the food material. In contrast, reflector type B (glossy surface), with a thawing time of approximately 18 min, ranked second. Although polished surfaces generally exhibit good reflectivity, they tend to have lower emissivity, and their specular (mirror-like) reflection may provide less uniform thermal coverage compared with diffuse reflection. Finally, reflector type C (mesh structure) demonstrated the weakest performance, with the longest processing time (approximately 22 min). The primary reason for this outcome is the reduction in effective reflective surface area and the loss of energy through the openings in the mesh structure. Therefore, for optimizing and accelerating the thawing process, the use of continuous matte surfaces appears to be preferable to polished or mesh configurations [15].

These findings are consistent with the results reported by Pezoban et al. (2020), who demonstrated that the matte surface of aluminum foil exhibits greater diffuse reflectivity, resulting in a more uniform redistribution of radiative energy. In contrast, the glossy surface of aluminum foil displays higher regular (specular) reflectivity, causing radiation to be reflected more directly and concentrically. These differences imply that matte surfaces distribute energy more uniformly, whereas glossy surfaces, due to mirror-like reflection, are more effective in concentrating light [16].

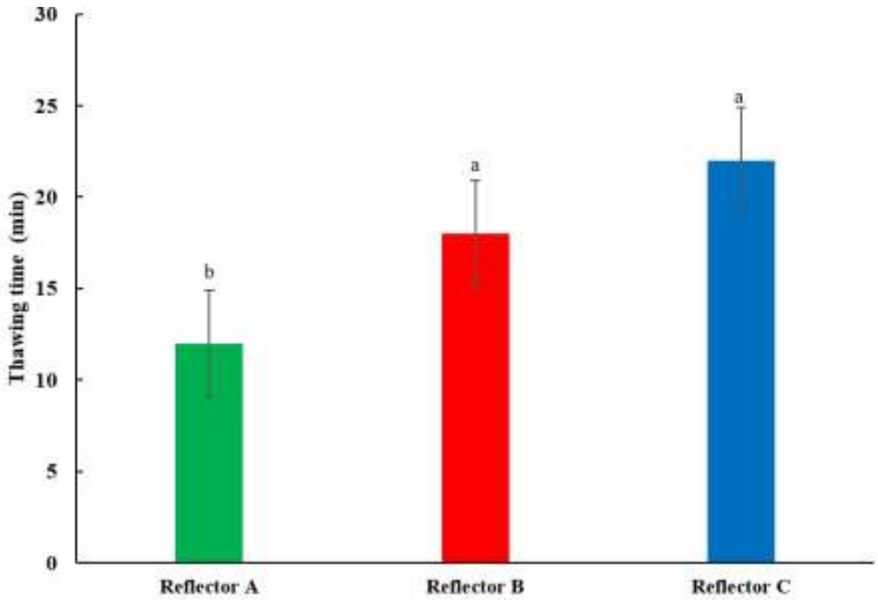


Figure 3. Thawing time of chicken meat under different reflectors.

Analysis of the temperature profiles of chicken samples during the thawing process (temperature profile curves) further confirmed the clear differences in heating rate and thermal behavior among the three reflector types (Figure 4). As shown in the graph, reflector A exhibited the steepest temperature rise, with the sample passing through the critical phase-change region (around 0ºC) in the shortest time and reaching the final temperature in approximately 10 minutes. This behavior indicates highly effective radiative heat transfer and a high level of energy absorption, which can be attributed to the matte nature of the reflector surface, resulting in a shortened phase-change period.

In contrast, reflector B showed intermediate behavior, while reflector C displayed the lowest heating rate and the longest residence time in the phase-change stage. The prolonged duration of this stage in the mesh reflector (C), mainly due to energy losses and the reduced effective reflective surface, is particularly important because extended exposure of the product within the temperature range of approximately -5 to 0 ºC increases the risk of protein structure degradation in chicken tissue. In contrast, the faster transition through this temperature range observed with reflector A provides more favorable conditions for preserving product quality [17].

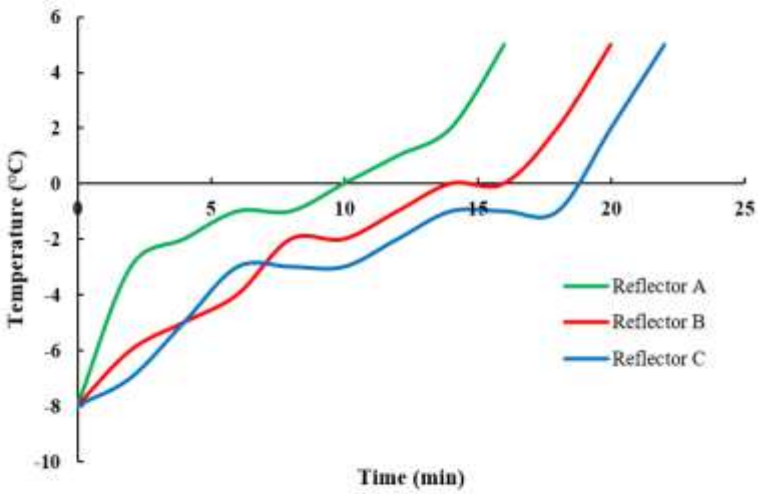


Figure 4. Temperature profile of chicken samples under different reflectors

### 3.2. Effect of Reflector Type on Weight Loss

Analysis of the weight loss results (Figure 5) indicates the presence of a relationship between the processing rate and the preservation of tissue moisture. Reflector type A (matte surface) showed the highest weight loss (approximately 2.25±3.1%)). This result suggests that the high intensity of radiative heat transfer and the high absorption coefficient of the matte surface led to a rapid increase in the temperature of the product's outer layer, thereby intensifying surface moisture evaporation.

In contrast, reflector type C (mesh structure) exhibited the lowest weight loss and therefore demonstrated better performance in preserving sample mass. Due to its porous structure and the associated energy losses, a milder heating rate was applied, preventing severe thermal shock and sudden evaporation of intercellular water; however, this occurred at the expense of a longer processing time. Reflector type B showed an intermediate condition, with a weight loss of approximately 1.8±0.24 %, indicating a balance between heat transfer and mass transfer phenomena.

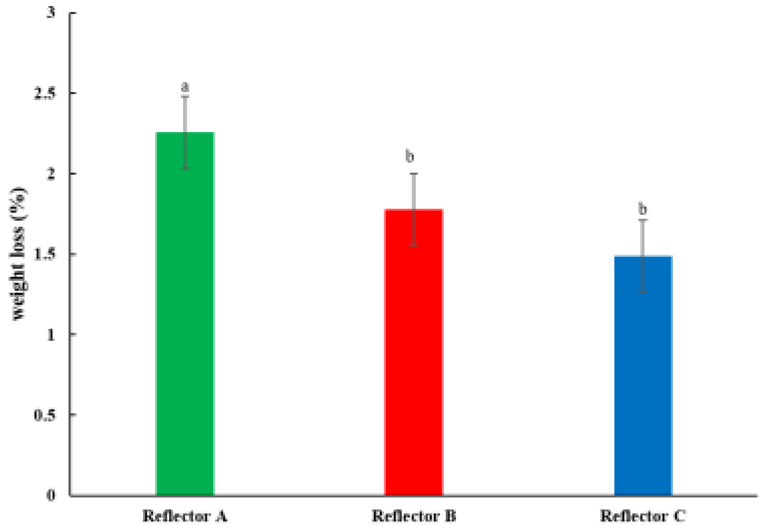


Figure 5. Weight loss in chicken meat under different reflectors

### 3.3. Effect of Reflector Type on Specific Energy Consumption

Evaluation of the specific energy consumption index revealed a direct correlation between process duration and energy efficiency. Reflector type A exhibited the lowest energy consumption (approximately 13.9±2.8 kJ/g), indicating the most optimal performance from both economic and thermodynamic perspectives. This high efficiency can be attributed to the ability of the matte surface to reflect thermal radiation effectively and uniformly, which significantly reduced the process time and consequently prevented prolonged operation of the energy source.

In contrast, reflector type C (mesh structure), with an energy consumption of approximately 24±3.1 kJ/g, nearly twice that of type A, was identified as the most energy-intensive option. This outcome can be explained by the unfavorable combination of energy leakage through the mesh openings and the extended processing time, both of which contributed to considerable energy losses. Reflector type B demonstrated an intermediate performance with a specific energy consumption of approximately 20±2.9 kJ/g. These results suggest that specular reflection is less efficient than diffuse reflection (matte surfaces) in converting input energy into useful heat within the food matrix (Figure 6).

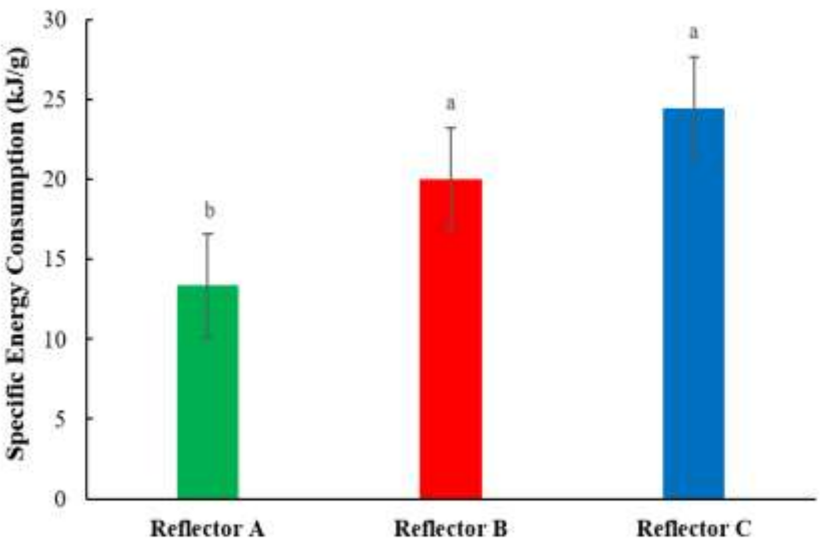


Figure 6. Specific energy consumption of chicken meat under different reflectors

**3.4. Effect of Reflector Type on Product Color**

Analysis of the colorimetric data, as a key indicator of the final product's visual quality, demonstrated a clear correlation with the heat-transfer and energy-consumption findings (Table 1). The matte reflector, through its diffuse reflection pattern and uniform distribution of heat flux across the sample surface, was able to maintain the lightness index ($L^*$) within 65.48±1.53, which is very close to the initial value of 66.75. This color stability reflects minimal thermal denaturation of myofibrillar proteins and effective prevention of oxidation of the heat-sensitive myoglobin pigments at the meat surface.

In contrast, samples treated with the glossy (specular) reflector, despite experiencing a more rapid heating rate, showed a sharp and significant reduction in the redness index ($a^*$) from 16.84±1.15 to 10.26±1.38. This undesirable effect is attributed to the nature of specular reflection, which creates localized hot spots. Concentration of energy in these zones leads to chemical degradation of the heme group in myoglobin or the leaching of water-soluble pigments through drip loss, both of which result in discoloration and reduced consumer appeal.

Finally, the mesh reflector produced the lowest final lightness values, yielding the darkest appearance among the treatments. This quality decline is linked to the extended thawing time required under this configuration, leaving the product surface exposed to air for longer. Prolonged exposure causes surface dehydration and the formation of a dry, darkened layer on the tissue [18].

Table 1. Color parameters of chicken samples (mean ± SD) under different reflector types.

| Parameter | Reflector Type | Before Freezing | After Thawing |
|---|---|---|---|
| $L^*$ (Lightness) | Reflector A (Matte) | $66.76 \pm 1.24^a$ | $65.48 \pm 1.53^a$ |
| $L^*$ (Lightness) | Reflector B (Polished) | $59.29 \pm 1.85^b$ | $58.26 \pm 2.12^b$ |
| $L^*$ (Lightness) | Reflector C (Mesh) | $34.75 \pm 1.60^c$ | $53.35 \pm 2.45^c$ |
| $a^*$ (Redness) | Reflector A (Matte) | $11.16 \pm 0.75^b$ | $13.84 \pm 0.92^b$ |
| $a^*$ (Redness) | Reflector B (Polished) | $16.84 \pm 1.15^a$ | $10.26 \pm 1.38^b$ |
| $a^*$ (Redness) | Reflector C (Mesh) | $16.78 \pm 1.10^a$ | $20.57 \pm 1.65^a$ |
| $b^*$ (Yellowness) | Reflector A (Matte) | $15.76 \pm 0.95^b$ | $16.87 \pm 1.18^b$ |
| $b^*$ (Yellowness) | Reflector B (Polished) | $22.66 \pm 1.40^a$ | $18.71 \pm 1.55^a$ |
| $b^*$ (Yellowness) | Reflector C (Mesh) | $12.89 \pm 0.85^b$ | $13.51 \pm 1.05^c$ |

### 3.5. Effect of Infrared Lamp Distance on Thawing Time and Temperature Profile

In this study, GAP—the distance between the infrared lamp and the meat surface—was examined as a key geometric parameter influencing the intensity of incident thermal radiation. The lamp–sample distance was set at three controlled levels (GAP-A: 14 cm, GAP-B: 17 cm, GAP-C: 20 cm) to evaluate its impact on thawing time, temperature profile, and quality attributes. Analysis of Figure 7 showed a non-linear response and the emergence of a saturation point in heat-transfer behavior. GAP-C produced the longest thawing time (≈14 minutes), significantly slower than the other treatments due to a sharp reduction in heat-flux density and the view factor, which decreases according to the inverse-square law and restricts the energy reaching the surface for rapid melting of ice crystals. The view factor ($F_{1\rightarrow2}$), a dimensionless geometric parameter, describes what fraction of emitted radiative energy directly reaches and is absorbed by the meat and determines the spatial uniformity of the absorbed heat-flux field. In contrast, the statistically similar thawing times of GAP-A and GAP-B (≈12 minutes) indicate that at shorter distances, external radiant intensity is no longer the limiting factor; instead, the rate is controlled by the internal conductive resistance of the meat, as the surface already receives sufficient energy to reach thermal saturation. Consequently, GAP-B (17 cm) represents the optimal operational distance, achieving the highest practical thawing rate without introducing risks of thermal stress or surface overheating that may occur at very short distances such as GAP-A.

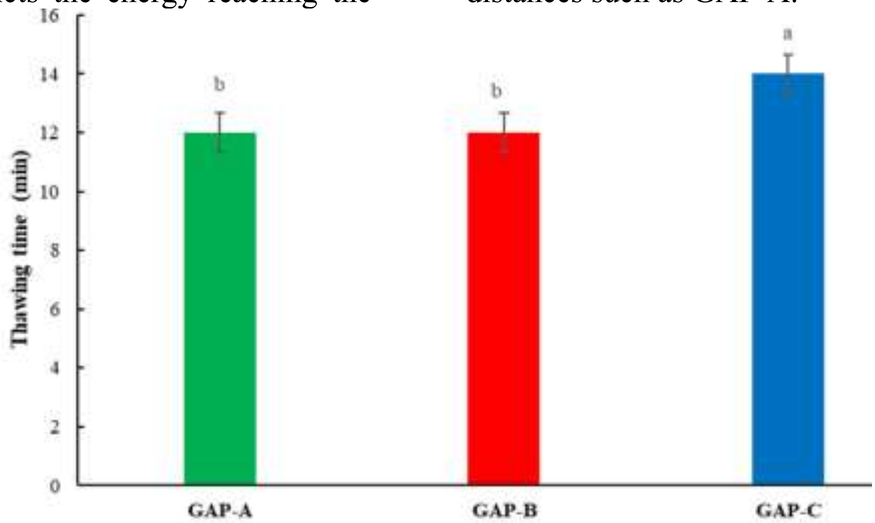


Figure 7. Thawing time of chicken meat at different distances from the infrared source

Thermal dynamic analysis of the thawing process based on the recorded temperature profiles (Figure 8) reveals fundamental differences in heat-transfer mechanisms at various lamp distances. The GAP-C treatment exhibited the longest and most extended phase-change plateau within the critical temperature range of −5 to 0 °C, indicating that the received heat flux was insufficient to rapidly overcome the latent heat of ice melting. This limitation slowed the process and prolonged the total thawing time to approximately 14 minutes. Although both GAP-A and GAP-B treatments reached the final target temperature in nearly 12 minutes, the characteristics of their heating trajectories differed substantially. The GAP-B profile displayed a smooth sigmoidal and continuous pattern, reflecting uniform heat penetration and a balanced interaction between incident radiative energy and internal conductive transfer. In contrast, the GAP-A curve showed a transient instability and a temporary reduction in temperature slope between 6 and 8 minutes. This non-linear behavior confirms the occurrence of surface thermal saturation and the formation of a thermally resistant superficial layer at very short distances, which hindered efficient heat transfer toward the geometric center of the sample. Therefore, the GAP-B profile represents the most stable thermodynamic pathway, achieving high thawing rates without inducing internal thermal shocks, and is consequently identified as the optimal operational condition. These findings are consistent with the thawing-time results discussed in the previous section.

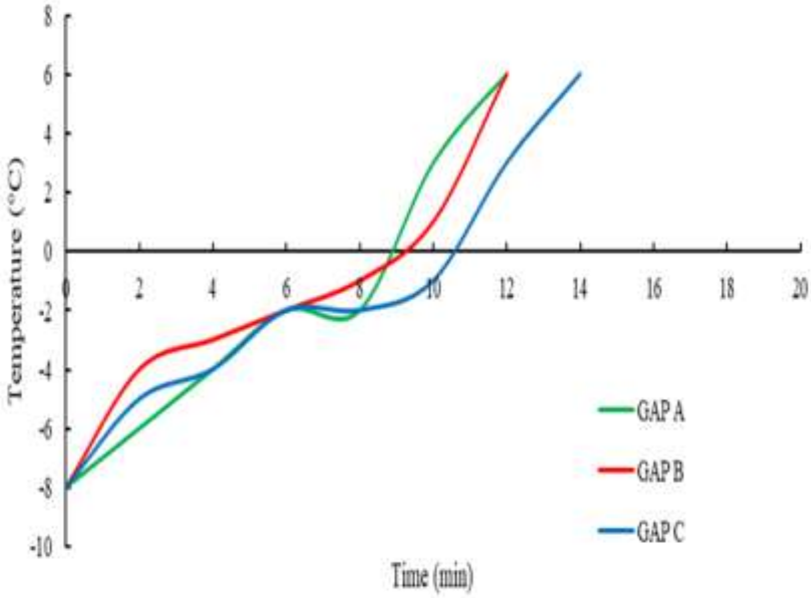


Figure 8. Temperature profile of chicken samples at different distance from infrared source

**3.6. Effect of Infrared Lamp Distance on Weight Loss**

Analysis of the weight-loss profile at different radiation-source distances (Figure 9) show a meaningful correlation with the previously discussed results on process time and temperature profiles, thereby supporting the proposed heat-transfer mechanisms. The GAP-C treatment exhibited the highest weight loss (approximately 3.00±0.34 %), representing the least favorable condition for moisture retention. From a technical standpoint, this outcome is closely associated with the prolonged process time (about 14 minutes) and the slow transition through the phase-change region at this distance. The extended exposure of the product to the surrounding environment and the delayed melting of ice crystals provided greater opportunity for surface evaporation and drip release resulting from structural damage in the tissue.

In contrast, GAP-A demonstrated the lowest weight loss (less than 1.7±0.41%), indicating that the higher heating rate at a shorter distance reduced the overall processing time and consequently limited mass transfer, leading to better moisture preservation. However, GAP-B, with a weight loss of approximately 2.20±0.44 %, occupied an intermediate position and presented a more balanced performance. Although its weight loss was slightly higher than that of GAP-A, considering the potential risk of thermal saturation and surface overheating at very short distances—observed in the temperature profile of GAP-A—this level of weight loss can be regarded as acceptable for achieving a more uniform and higher-quality thawing process.

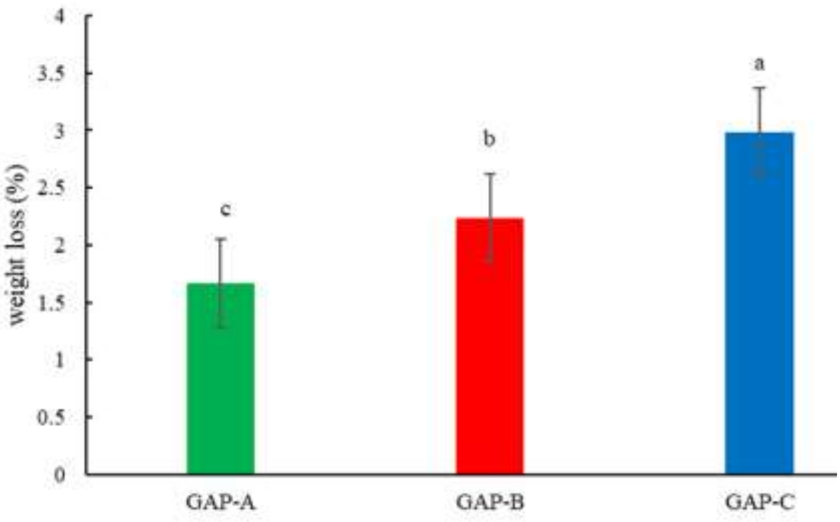


Figure 9. Weight loss in chicken meat at different distances from the infrared source.

**3.7. Effect of Infrared Lamp Distance on Specific Energy Consumption**

Analysis of the specific energy consumption profile (Figure 10) reveals a clear and nearly linear relationship between process duration and energy efficiency, further confirming the findings obtained from thawing time and temperature-profile analyses. The GAP-C treatment recorded the highest specific energy consumption, approximately 20±2.2 kJ/g, indicating the lowest thermodynamic efficiency among the tested conditions ($P < 0.01$). This considerable increase in energy demand is primarily attributed to the extended processing time at this distance. As the lamp–sample distance increases, the view factor and radiation intensity decrease, requiring the system to operate for a longer period to supply the enthalpy necessary for ice melting. Consequently, a significant portion of the input electrical energy is dissipated as thermal losses rather than being effectively utilized for phase change.

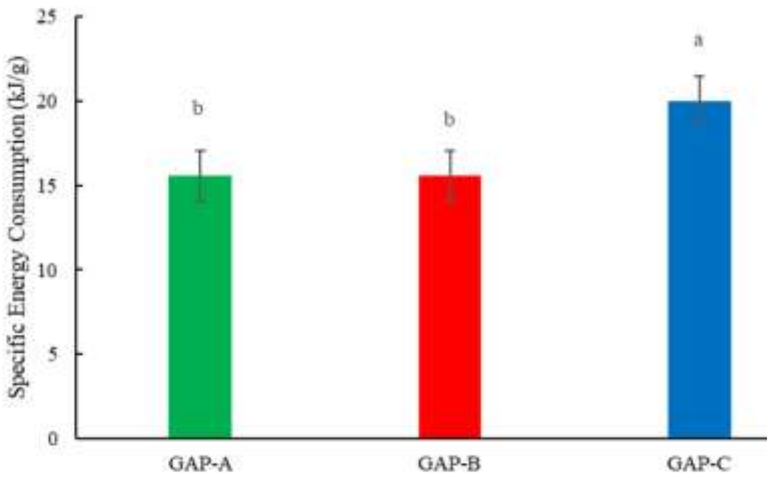


Figure 10. Specific energy consumption of chicken meat at different distances from the infrared source.

In contrast, GAP-A and GAP-B showed statistical overlap, both falling within the range of approximately 15±1.5 to 16±1.4 kJ/g and sharing the same significance group (b). This result indicates that reducing the distance from 17 cm to 14 cm does not yield additional energy savings, suggesting that the system has already reached its maximum energy-absorption efficiency. Therefore, considering that GAP-B provides nearly the same energy efficiency as GAP-A while avoiding the potential quality risks observed at shorter distances—such as surface overheating and thermal saturation—the 17 cm distance can be identified as the optimal eco-thermodynamic operating point, offering minimal energy consumption while maintaining superior product quality [21].

### 3.8. Effect of Infrared Lamp Distance on Product Color

Comprehensive analysis of the colorimetric data provides additional evidence confirming the heat- and mass-transfer mechanisms occurring at different infrared source distances (Table 2). At the optimal distance of 17 cm, the stability of the lightness ($L^*$) and yellowness ($b^*$) parameters, with minimal deviation from the fresh sample, indicates a uniform distribution of heat flux and effective penetration of thermal energy into the product. Such conditions prevent the formation of steep thermal gradients on the surface and consequently limit thermal denaturation of myofibrillar proteins as well as undesirable Maillard reactions or oxidative processes that lead to color degradation.

In contrast, the most pronounced quality deterioration occurred at the 20 cm distance, where a significant increase in the yellowness index (26.48$\pm$1.80) was observed. This phenomenon is strongly correlated with the highest weight loss and the longest processing time recorded at this distance. Prolonged exposure to atmospheric oxygen and extensive surface evaporation promotes surface dehydration, concentration of heme pigments, and accelerated lipid oxidation, ultimately resulting in a darker and more yellowish appearance of the tissue [22].

At the 14 cm distance, despite the shorter overall process time, a reduction in the lightness index was also detected. This behavior suggests the occurrence of surface thermal saturation caused by excessive radiation intensity in the near-field region. In this situation, energy concentration exceeds the internal heat-conduction capacity of the tissue, initiating structural alterations and localized surface scorching.

Table 2. Color parameters of chicken samples (mean ± SD) under different distances from the infrared source.

| **Parameter** | **Distance** | **Before Freezing** | **After Thawing** |
|---|---|---|---|
| $L^*$ (Lightness) | 14 cm | $61.49 \pm 1.85^b$ | $57.30 \pm 2.10^b$ |
| $L^*$ (Lightness) | 17 cm | $58.04 \pm 1.60^c$ | $56.33 \pm 1.95^b$ |
| $L^*$ (Lightness) | 20 cm | $65.12 \pm 1.90^a$ | $59.15 \pm 2.25^a$ |
| $a^*$ (Redness) | 14 cm | $17.82 \pm 1.10^b$ | $18.09 \pm 1.35^b$ |
| $a^*$ (Redness) | 17 cm | $23.85 \pm 1.45^a$ | $22.26 \pm 1.50^a$ |
| $a^*$ (Redness) | 20 cm | $13.80 \pm 1.20^c$ | $18.29 \pm 1.60^b$ |
| $b^*$ (Yellowness) | 14 cm | $20.85 \pm 1.30^b$ | $22.65 \pm 1.55^b$ |
| $b^*$ (Yellowness) | 17 cm | $23.61 \pm 1.40^a$ | $23.88 \pm 1.70^b$ |
| $b^*$ (Yellowness) | 20 cm | $19.89 \pm 1.25^b$ | $26.48 \pm 1.80^a$ |

## 4- Conclusion

The findings of this study demonstrate that accelerating the phase-change process while preserving the quality of chicken meat is achievable, provided that the geometric configuration of the system is optimized to overcome limitations associated with thermal penetration. Analysis of the results showed that the use of matte reflectors, compared with polished (glossy) surfaces used as the ground electrode, is preferable because diffuse reflection distributes energy more uniformly across the irregular topography of the product. This uniform distribution prevents localized thermal stress that can lead to protein denaturation and reduction of the redness index.

The results also indicate that reducing the radiation-source distance does not necessarily accelerate the thawing process. At a distance of 14 cm, the rate of energy input exceeds the thermal conduction capacity of the tissue, leading to surface thermal saturation and consequently slowing heat transfer toward the thermal center of the sample. In contrast, adjusting the distance to 17 cm improves the uniformity of the view factor, creating an optimal balance between radiative heat transfer and mass transfer (surface evaporation). This condition results in minimal weight loss and improved color stability.

Overall, the proposed hybrid thawing system operating under optimal conditions (matte reflector with a 17 cm lamp distance) significantly reduces processing time and energy consumption compared with conventional thawing methods and even with non-optimized modern configurations. Therefore, it can be considered a promising and intelligent industrial approach for enhancing food safety and reducing losses within the poultry meat supply chain.

## Data Availability

The datasets generated and/or analyzed during this study are available from the corresponding author upon reasonable request.

## Conflict of Interest

The authors declare that they have no known competing financial interests or personal relationships that could have appeared to influence the work reported in this paper.

## Funding Statement

This research was financially supported by the Iran National Science Foundation (INSF) under grant number 4045173.

## Author Contributions

**Mohsen Dalvi-Isfahan:** Supervision, project administration, conceptualization, validation, writing – review and editing.

**Hamid Khafajeh:** Methodology, formal analysis, data curation, writing – original draft.

# 5-References

[1] Agricultural Statistics Yearbook (2024). Office of Statistics and Information Technology, Ministry of Agriculture Jihad, Iran [In Persian].

[2] Leygonie C., Britz, T. J., & Hoffman, L. C. (2012). Impact of freezing and thawing on the quality of meat: Review. *Meat Science*, 91(2), 93-98.

[3] Dalvi-Isfahan M., Hamdami, N., Xanthakis, E., & Le-Bail, A. (2017). Review on the control of ice nucleation by ultrasound waves, electric and magnetic fields. *Journal of Food Engineering*, 195, 222-234.

[4] Acheampong R., Osei Tutu, C., Akonor, P. T., Asiedu, B. K., Mahama, S., Owusu-Bempah, J., Appiadu, D., Koranteng, A. F., Kumador, D. K., Andoh-Odoom, A. H., & Kwesi Saalia, F. (2025). Effect of conventional and emerging thawing technologies on drip loss, microstructure and post-thaw quality of frozen fruits and vegetables: A review. *Applied Food Research*, 5(2), 101323.

[5] He X., Liu, R., Nirasawa, S., Zheng, D., & Liu, H. (2013). Effect of high voltage electrostatic field treatment on thawing characteristics and post-thawing quality of frozen pork tenderloin meat. *Journal of Food Engineering*, 115(2), 245-250.

[6] Rahbari M., Hamdami, N., Mirzaei, H., Jafari, S. M., Kashaninejad, M., & Khomeiri, M. (2018). Effects of high voltage electric field thawing on the characteristics of chicken breast protein. *Journal of Food Engineering*, 216, 98-106.

[7] Mousakhani-Ganjeh A., Hamdami, N., & Soltanizadeh, N. (2016). Effect of high voltage electrostatic field thawing on the lipid oxidation of frozen tuna fish (*Thunnus albacares*). *Innovative Food Science & Emerging Technologies*, 36, 42-47.

[8] Sheridan P., & Shilton, N. (1999). Application of far infra-red radiation to cooking of meat products. *Journal of Food Engineering*, 41(3), 203-208.

[9] Davoudi, M.; Kashani-Nejad, M.; Ziaei-Far, A. M.; Ghorbani, M. (2018). Optimization of thawing of ground chicken by infrared radiation- warm air method using response surface methodology. *Iranian Food Science and Technology Research Journal*, 14(4), 461–472. [In Persian].

[10] Dalvi-Isfahan M., Havet, M., Hamdami, N., & Le-Bail, A. (2023). Recent advances of high voltage electric field technology and its application in food processing: A review with a focus on corona discharge and static electric field. *Journal of Food Engineering*, 353, 111551.

[11] Misra N. N., Martynenko, A., Chemat, F., Paniwnyk, L., Barba, F. J., & Jambrak, A. R. (2018). Thermodynamics, transport phenomena, and electrochemistry of external field-assisted nonthermal food technologies. Critical Reviews in Food Science and Nutrition, 58(11), 1832-1863.

[12] Martynenko A. (2025). EHD-induced mass transfer from wet materials. *Journal of Electrostatics*, 137, 104075.

[13] Maleki-Bohlooli Z., Dalvi-Isfahan, M., Elmizadeh, A., Taghipour, L., & Mohtashami, S. (2025). Comparative effects of cold plasma and high-voltage electric field on physicochemical changes in persimmon during storage. *Applied Food Research*, 5(2), 101171.

[14] Majid M., Fallah-Joshaqani, S., Dalvi-Isfahan, M., & Hamdami, R. (2023). Comparison of Conventional and Microwave-assisted Extraction of Pectin from Watermelon Rind. *Journal of Polymers and the Environment*, 31(8), 3363-3371.

[15] Xie F., Jiang, F., Niu, J., Yu, Q., & Yuan, Y. (2025). Effect of surface emissivity on the aerothermodynamics of the evacuated tube transportation. *Thermal Science and Engineering Progress*, 65, 103892.
[16] Pozzobon V., Levasseur, W., Do, K.-V., Palpant, B., & Perré, P. (2020). Household aluminum foil matte and bright side reflectivity measurements: Application to a photobioreactor light concentrator design. *Biotechnology Reports*, 25, e00399.
[17] Fellows P. J. (2017). 22 - Freezing. In P. J. Fellows (Ed.), *Food Processing Technology* (Fourth Edition) (pp. 885-928): Woodhead Publishing.
[18] Zhu Y., Zhu, J., Shi, X., & Fan, M. (2025). Effects of Freezing, Frozen Storage and Thawing on the Water Status, Quality, Nutrition and Digestibility of Meat: A Review. *Food Science & Nutrition*, 13(8), e70774.
[19] Fakayode O. A., Ojoawo, O. O., Zhou, M., Wahia, H., & Ogunlade, C. A. (2025). Revolutionizing food processing with infrared heating: New approaches to quality and efficiency. *Food Physics*, 2, 100046.
[20] Tanaka F., Verboven, P., Scheerlinck, N., Morita, K., Iwasaki, K., & Nicolaï, B. (2007). Investigation of far infrared radiation heating as an alternative technique for surface decontamination of strawberry. *Journal of Food Engineering*, 79(2), 445-452.
[21] Aboud S. A., Altemimi, A. B., A, R. S. A.-H., Yi-Chen, L., & Cacciola, F. (2019). A Comprehensive Review on Infrared Heating Applications in Food Processing. *Molecules*, 24(22).
[22] Dalvi-Isfahan M., Hamdami, N., & Le-Bail, A. (2016). Effect of freezing under electrostatic field on the quality of lamb meat. *Innovative Food Science & Emerging Technologies*, 37, 68-73.

مجله علوم و صنایع غذایی ایران

سایت مجله: www.fsct.modares.ac.ir

مقاله علمی_پژوهشی

# مطالعه تجربی رفع انجماد گوشت مرغ با استفاده از فناوری تلفیقی میدان الکتریکی و مادون قرمز (بررسی اثر تأثیر پیکربندی بازتابنده و فاصله از منبع نوری)

محسن دلوی-اصفهان[1*]، حمید خفاجه[2*]

۱-دانشیار گروه علوم و صنایع غذایی، دانشکده کشاورزی، دانشگاه جهرم، جهرم، ایران

۲-استادیار گروه مهندسی مکانیک بیوسیستم، دانشکده کشاورزی، دانشگاه جهرم، جهرم، ایران

اطلاعات مقاله

تاریخ های مقاله :

تاریخ دریافت: ۱۴۰۴/۱۲/۰۶

تاریخ داوری: ۱۴۰۵/۰۲/۲۳

تاریخ پذیرش: ۱۴۰۵/۰۲/۳۰

کلمات کلیدی:

رفع انجماد،

میدان الکتریکی،

مادون قرمز،

گوشت مرغ،

کیفیت بافت،

انرژی مصرفی ویژه.

DOI: 10.48311/fsct.2026.119582.83083

* مسئول مکاتبات:

Dalvi@jahromu.ac.ir,
mohsen.Dalvi@gmail.com

khafajeh@jahromu.ac.ir

چکیده

در این پژوهش، برای رفع محدودیت‌های انتقال حرارت هدایتی، کارایی یک سامانه هیبریدی شامل تابش مادون‌قرمز و میدان الکتریکی با شدت ٦/٧ کیلوولت بر سانتی‌متر در رفع انجماد فیله مرغ منجمد بررسی شد. متغیرهای مورد مطالعه شامل نوع بازتابنده (مات، براق و مشبک) و فاصله منبع تابش در سه سطح بود و تأثیر آنها بر سینتیک حرارتی، انرژی مصرفی ویژه، افت وزن و مؤلفه‌های رنگ ارزیابی گردید. نتایج نشان داد ویژگی‌های اپتیکی بازتابنده نقش مهمی در یکنواختی شار حرارتی دارند. بازتابنده مات با ایجاد بازتاب پخشی، زمان رفع انجماد را به حدود ١٢ دقیقه و مصرف انرژی را به ١٣ کیلوژول بر گرم کاهش داد و با جلوگیری از تشکیل نقاط داغ، روشنایی سطح را حفظ کرد. در مقابل، بازتابنده مشبک به‌دلیل اتلاف انرژی بیشتر، زمان فرایند را به حدود ٢٢ دقیقه افزایش داد. همچنین، شدت بالاتر انتقال حرارت تابشی در بازتابنده مات موجب بیشترین افت وزن شد، در حالی‌که بازتابنده مشبک با گرمایش ملایم‌تر، کمترین افت وزن و حفظ بهتر رطوبت را نشان داد. بررسی فاصله منبع تابش نیز رفتار غیرخطی وابسته به ضریب دید را آشکار کرد. فاصله ١٤ سانتی‌متر به‌دلیل اشباع حرارتی موجب کاهش کیفیت رنگ گردید، اما فاصله ١٧ سانتی‌متر با ایجاد تعادل میان شدت تابش و نفوذ حرارت، ضمن حفظ رنگ و حداقل افت وزن، به‌عنوان فاصله بهینه تعیین شد. در مجموع، ترکیب بازتابنده مات و فاصله ١٧ سانتی‌متر کارآمدترین شرایط اکوترمودینامیکی را فراهم نمود.